CHEMISTRY & BIODIVERSITY

Accepted Article

Title: Synthesis, Biological Activity and Action Mechanism Study of Novel Chalcone Derivatives Containing Malonate

Authors: Tao Guo, Rongjiao Xia, Tingting Liu, Feng Peng, Xuemei Tang, Qing Zhou, Hui Luo, and Wei Xue

To be cited as: *Chem. Biodiversity* 10.1002/cbdv.202000025

Link to VoR: http://dx.doi.org/10.1002/cbdv.202000025

Chem. Biodiversity

Synthesis, Biological Activity and Action Mechanism Study of Novel Chalcone Derivatives Containing Malonate

Tao Guo, Rongjiao Xia, Tingting Liu, Feng Peng, Xuemei Tang, Qing Zhou, Hui Luo, Wei Xue*

State Key Laboratory Breeding Base of Green Pesticide and Agricultural Bioengineering;
Center for Research and Development of Fine Chemicals, Guizhou University, G uiyang 550025, P.R. China.
e-mail:wxue@gzu.edu.cn

Abstract

A series of novel chalcone malonate derivatives were synthesized and their antibacterial and antiviral activities were evaluated. All target compounds were characterized by spectral data. The results of antimicrobial bioassay showed that compound **3e** showed excellent antibacterial activity against Xanthomonas oryzae pv oryzae (Xoo), with an EC50 value of 10.2 μg/mL, which is significantly superior to bismerthiazol (71.7 μg/mL) and thiodiazole copper (97.8 μg/mL). At the same time, the mechanism of **3e** and **3k** was confirmed by scanning electron microscopy. In addition, compound **3g** showed significant curative activity to tobacco mosaic virus, with a value of 74.3%, which was superior to 53.3% of ningnanmycin. The results of microscale thermophoresis also showed that the Kd value of the combination of **3b** and **3g** with the coat protein of tobacco mosaic virus was 0.211 and 0.166 μmol / L, which was better than 0.596 μmol / L of ningnanmycin. At the same time, the molecular docking of **3b** and **3g** with tobacco mosaic virus-coat protein shows that the compound is well embedded in the pocket between the two subunits of tobacco mosaic virus-coat protein. These results show that chalcone derivatives containing malonate group can be considered as activators in the design of antibacterial and antiviral agents.

Keywords: Chalcone • Malonate • Biological activity • Action mechanism

Introduction

Plant diseases are usually caused by invasive plant pathogens and are widespread and toxic, seriously threatening agricultural output and the quality of global agricultural production; moreover, they have become one of the most important problems in agricultural production.[1-4] One of the world famous rice pathogens-*Xanthomonas oryzae pv oryzae* (Xoo) is an excessive albinism that occurs during any rice growth period. In the case of the occurrence and spread of this disease, it may result in a substantial reduction of production by up to 80 %.[5-8] *Ralstonia solanacearum* (Rs) bacterial wilt is the most important bacterial disease that damages tobacco, and important cash crops such as tobacco, tomato, peanut and potato are seriously damaged.[9-10] Citrus bacterial canker, which is caused by a severe and widespread Gram-negative pathogen *Xanthomonas axonopodis pv. Citri* (Xac), It is a highly toxic disease. The disease occurs on leaves, twigs, thorns, old branches and fruits, causing falling fruits and fallen leaves.[11-12] These bacteria can actively suppress the crop yields worldwide. Virus in plants, known as plant cancer, are very difficult to control once plants have been infected, and give rise to serious damage. As an example, tobacco mosaic virus is the most persistent plant virus and can survive in dry plant debris for up to 100 years. Individuals in more than 100 plant families can infect the virus, significant loss of crops each year globally due to plant diseases caused by tobacco mosaic virus.[13-15] Hence, the development of novel anti-viral molecules against tobacco mosaic virus has attracted an increasing amount of attention. To overcome these serious problems, antibacterial drugs such as bismerthiazol, thiodiazole copper, and ningnanmycin have been widely developed and used to reduce the infection of bacteria and plant viruses.[16-17] However, the long-term non-standard use of traditional anti-phytopathogenic drugs has led to increased resistance to plant pathogenic genes, which not only enhanced the resistance of target pathogens, but also caused serious damage to plant growth systems.[18-20] Therefore, it is necessary to research and create a new simple structure with high biological activity and low toxicity as an alternative fungicide, which is also an important task in the research and development process of pesticides.

Chalcone is a kind of natural organic substance found in medicinal plants such as licorice and safflower. It has low toxicity and low residue, and it has different flexibility due to its molecular structure.[21-23] Combined, it exhibits a wide range of biological activities such as antibacterial,[24,25] insecticidal,[26,27] anticancer,[28] antiviral,[29,30] anti-inflammatory[31] and other biological activities. Therefore, chalcone has potential research value in the field of new pesticide synthesis. Malonate compounds are important raw materials for the synthesis of many pharmaceutical intermediates[32] and their pharmacologically effective groups also have antibacterial,[33] antiviral,[34,35] anticancer,[36] anti-inflammatory[37] and other biological activities.

In order to find small organic pesticides with high biological activity and low toxicity, a series of new organic small molecules were designed and synthesized by combining the malonic acid group with excellent biological activity and chalcone structure by splicing. Through biological activity

screening, it is expected to find chalcone compounds with high bacteriostatic and anti-plant virus activity, which provides a certain basis for the development of new pesticides.

Graphical Abstract

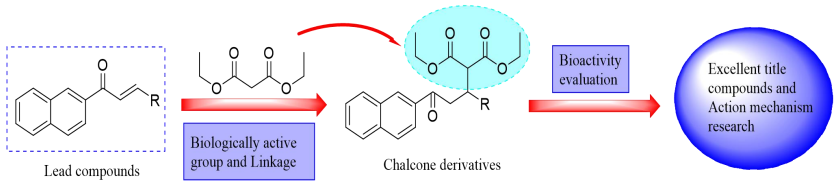

Results and Discussion

Chemistry

The structures of all compounds were confirmed by nuclear magnetic resonance (NMR) and high resolution mass spectrometry (HRMS), and the spectra data are shown in the Supplementary Materials. Representative data for **3a** are listed below. In 1H NMR spectra, multiplet signals at δ 8.65-7.33 ppm indicate the presence of protons in olefinic bonds and aromatic nuclei, and two singlets at δ 1.19 and 0.93 ppm indicate the presence of -CH_3 groups.The ^{13}C NMR spectra of the **3a** exhibited a characteristic (C=O) signal at δ 197.92, 168.23 and 167.74 ppm. Absorption signals at δ 14.29 and 13.29 ppm in ^{13}C NMR spectra confirm the presences of -CH_3 groups. The strong presence of $[M+H]^+$ ions indicates that the title compounds are in the steady state.

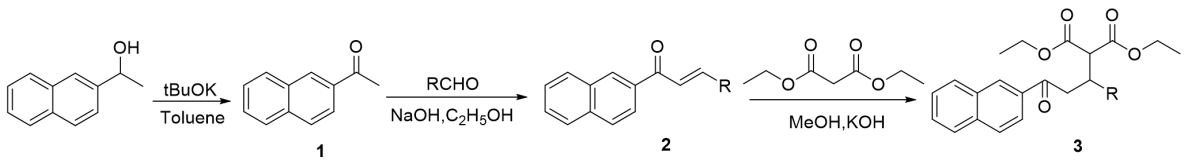

3a: R= 4-Cl-Ph; **3b**: R= 4-F-Ph; **3c**: R= 2-Cl-Ph; **3d**: R= 4-CH_3-Ph;
3e: R= 3-NO_2-Ph; **3f**: R= 4-OCH_3-Ph; **3g**: R= 4-NO_2-Ph; **3h**: R= 2-F-Ph;
3i: R= 3-CH_3-Ph; **3j**: R= 3-Br-Ph; **3k**: R= 4-Br-Ph; **3l**: R= 2,6-di-Cl-Ph;
3m: R= 4-C_3H_7-Ph; **3n**: R= 2-Thiophene; **3o**: R= 2-Furan;

Scheme 1. The synthesis of target compounds

Antibacterial activity of target compounds against Xac, Xoo and Rs in vitro

The antibacterial activity of the synthesized target compounds **3a-3o** against three common plant pathogenic bacteria (Xac, Xoo and Rs) was determined by turbidimetry. Use the commonly used bactericides (thiodiazole copper and bismerthiazol) as controls. As shown in Table 1, some compounds have significant antibacterial activity against Xac, Xoo and Rs at concentrations of 100 or 50 μg/mL, exceeding the control bactericides. Highly active compounds in bacteriostatic tests, **3c**、**3d**、**3e**、**3k**、**3l** against Xac at 100 μg/mL were 95.5、98.0、87.0、98.9、97.2 %, the two control fungicides thiodiazole copper (57.2%) and bismerthiazol (65.3%) were exceeded, respectively. Compounds **3a**、**3c**、**3e**、**3f**、**3g**、**3h**、**3j**、**3k**、**3l** against Xoo at 100 μg/mL were 85.2、72.6、98.6、78.3、72.3、70.1、93.2、89.4、87.2 %, respectively, which were better compared to thiodiazole copper (50.2 %) and bismerthiazol (64.9 %). In particular, the antibacterial activities of the compounds **3f**、**3j**、**3l** against Rs at 100 and 50 μg/mL were 98.5 and 62.6 %, 97.7 and 59.2 %, 95.6 and 52.6 %, respectively, which were significantly superior to thiodiazole copper (45.2 and 20.6 %) and bismerthiazol (53.7 and 32.2 %).

Under preliminary screening at concentrations of 100 and 50 μg/mL respectively, some target compounds with high activity were selected and their EC50 values were determined to further confirm that the selected compounds have excellent antibacterial activity. The EC50 results obtained are shown in Table 2. Compounds **3c**、**3d**、**3e**、**3k**、**3l** exhibited remarkable antibacterial activities against Xac, with EC_{50} values of 20.2、19.0、26.4、10.3、18.3 μg/mL, which were much better compared to thiodiazole copper (94.7 μg/mL) and bismerthiazol (51.6 μg/mL). Compounds **3a**、**3e**、**3j**、**3k**、**3l** exhibited excellent antibacterial activities against Xoo, with EC_{50} values of 29.4、10.2、23.4、29.6、32.3 μg/mL, respectively which were significantly superior to thiodiazole copper (97.8 μg/mL) and bismerthiazol (71.7 μg/mL). Compounds **3f**、**3j**、**3k**、**3l** exhibited notable antibacterial activities against Rs, with EC_{50} values of 11.2、11.6、19.3、16.8 μg/mL, respectively, which were much better than thiodiazole copper (78.8 μg/mL) and bismerthiazol (98.6 μg/mL). These antibacterial test results indicate that when looking for new organic small-molecule antibacterial agents, such compounds as malonate-containing chalcone should be further studied as potential biocide substitute templates, and there is room for further research.

Table 1. Antibacterial activities of title compounds (**3a–3o**) against plant pathogens Xac, Xoo and Rs in vitro.

Compounds	R	Xac /%		Xoo /%		Rs /%	
		100 μg/mL	50 μg/mL	100 μg/mL	50 μg/mL	100 μg/mL	50 μg/mL
3a	4-Cl-Ph	60.1±1.6	25.4±3.3	85.2±2.3	42.1±3.8	44.9±1.9	26.4±3.2
3b	4-F-Ph	59.3±2.5	22.6±3.4	44.9±1.3	24.3±1.4	23.1±2.1	11.2±4.5
3c	2-Cl-Ph	95.5±3.5	53.5±5.0	72.6±2.1	39.7±3.2	73.8±2.9	45.2±1.6
3d	4-CH_3-Ph	98.0±4.8	39.7±2.2	42.7±4.2	20.8±3.8	78.5±1.4	45.2±2.7
3e	3-NO_2-Ph	87.0±3.4	51.7±3.6	98.6±1.5	50.2±2.9	75.9±0.9	39.7±2.6
3f	4-OCH_3-Ph	35.2±1.7	20.8±2.9	78.3±3.8	38.7±1.3	98.5±1.7	62.6±0.5
3g	4-NO_2-Ph	49.3±1.8	26.3±1.7	72.3±2.8	32.9±4.2	35.4±1.9	17.5±2.9
3h	2-F-Ph	52.5±2.9	31.9±2.1	70.1±0.9	32.7±2.8	55.2±3.7	32.5±1.3
3i	3-CH_3-Ph	28.3±2.7	13.2±0.9	68.2±2.8	38.4±3.1	32.1±4.5	19.3±2.0
3j	3-Br-Ph	60.5±4.3	31.2±2.7	93.2±4.9	49.2±1.1	97.7±2.4	59.2±1.6
3k	4-Br-Ph	98.9±4.8	47.6±3.4	89.4±2.6	41.5±4.4	82.1±5.2	36.8±2.8
3l	2,4-di-Cl-Ph	97.2±1.5	45.2±2.9	87.2±1.7	41.2±2.0	95.6±2.2	52.6±2.9
3m	4-C_3H_7-Ph	48.2±1.7	24.9±4.2	53.2±3.8	27.9±0.7	60.5±1.7	28.8±4.6
3n	2-Thiophene	35.3±1.8	18.5±3.9	45.2±2.7	28.3±4.9	67.6±2.0	36.4±4.2
3o	2-Furan	31.2±1.2	14.9±3.9	68.1±1.8	32.1±4.7	52.7±0.9	21.7±3.7
TC[a]	-	57.2±1.3	27.8±3.8	50.2±0.9	37.2±3.2	45.2±4.3	20.6±2.7
BT[a]	-	65.3±2.8	54.9±5.5	64.9±3.9	45.2±2.0	53.7±3.6	32.2±2.8

[a] The commercial agricultural antibacterial agents Thiodiazole copper (TC) and Bismerthiazol (BT) were used as control agents.

Table 2. EC_{50} values of the title compounds against plant pathogenic bacteria in vitro.

Bacterial	Compounds	R	Toxic Regression Equation	r	EC_{50}/(μg/mL)
Xac	**3c**	2-Cl-Ph	y=2.0441x+2.3315	0.9781	20.2
	3d	4-CH_3-Ph	y=2.1777x+2.2161	0.9683	19.0
	3e	3-NO_2-Ph	y=1.8679x+2.3444	0.9938	26.4
	3k	4-Br-Ph	y=1.9909x+2.9847	0.9574	10.3
	3l	2,4-di-Cl-Ph	y=2.0990x+2.3484	0.9628	18.3
	TC[a]	-	y=1.1576x+2.7122	0.9859	94.7
	BT[a]	-	y=1.0698x+3.1679	0.9831	51.6
Xoo	**3a**	4-Cl-Ph	y=1.4470x+2.8757	0.9560	29.4
	3e	3-NO_2-Ph	y=1.7574x+3.2242	0.9579	10.2
	3j	3-Br-Ph	y=2.1632x+2.0375	0.9956	23.4
	3k	4-Br-Ph	y=1.9746x+2.0938	0.9874	29.6
	3l	2,4-di-Cl-Ph	y=1.9627x+2.0382	0.9904	32.3
	TC[a]	-	y=1.2058x+2.2869	0.9971	97.8
	BT[a]	-	y=0.9913x+3.1606	0.9802	71.7
Rs	**3f**	4-OCH_3-Ph	y=2.0600x+2.8395	0.9579	11.2
	3j	3-Br-Ph	y=1.7958x+3.0902	0.9814	11.6
	3k	4-Br-Ph	y=1.1995x+3.4570	0.9958	19.3
	3l	2,4-di-Cl-Ph	y=1.7653x+2.8363	0.9659	16.8
	TC[a]	-	y=1.4682x+1.8274	0.9758	78.8
	BT[a]	-	y=1.2581x+2.4918	0.9746	98.6

[a] The commercial agricultural antibacterial agents Thiodiazole cpper (TC) and Bismerthiazol (BT) were used as control agents.

Structure-activity relationships of antibacterial activities

The antibacterial test shows that the different substituents of the same parent compound affect the antibacterial biological activity of the compound. The differences in structure and activity are discussed below. For instance, the designated compounds **3c** (R=2-Cl-Ph), **3d** (R=4-CH_3-Ph), **3e** (R=3-NO_2-Ph), **3k** (R=4-Br-Ph) and **3l** (R=2,4-di-Cl-Ph) exhibited significant anti Xac at 100 μg/mL, with the inhibition rates of 95.5、98.0、87.0、98.9、97.2 %, respectively. Compounds with these substituents were found to be more antibacterial than compounds containing other substituents. However, when substituent R was substituted with 4-Cl-Ph, 2-Cl-Ph、3-NO_2-Ph、4-OCH_3-Ph、4-NO_2-Ph、2-F-Ph、3-Br-Ph、4-Br-Ph、2,4-di-Cl-Ph groups, the activities of the corresponding compounds **3a**、**3c**、**3e**、**3f**、**3g**、**3h**、**3j**、**3k**、**3l** against Xoo at 100 μg/mL were 85.2、72.6、98.6、78.3、72.3、70.1、93.2、89.4、87.2 %, respectively, which were significantly higher than that of bismerthiazol (64.9 %) and thiadiazole-copper (50.2 %). Notably, when substituent R groups was 2-Cl-Ph (**3c**)、4-CH_3-Ph (**3d**)、3-NO_2-Ph (**3e**)、4-OCH_3-Ph (**3f**)、3-Br-Ph (**3j**)、4-Br-Ph (**3k**)、2,4-di-Cl-Ph (**3l**) at a concentration of 100 μg/mL , it has significant anti-Rs biological activity, inhibition rates of 73.8、78.5、75.9、98.5、97.7、82.1、95.6 %, respectively.

Scanning electron microscopy (SEM) study

Based on the results of the target compounds **3a-30** resistance to plant pathogens (Tables 1 and 2), the two compounds with the most significant activity were selected, and the antibacterial action mechanism of the two plant bacteria Xac and Xoo was initially analyzed and studied by scanning electron microscopy. It can be seen that the compound damages the cell membrane of plant pathogens, and when the concentration of the compound is increased, it further affects the plant bacteria, and the cell membrane of the bacteria is more severely damaged, even passing through the cell membrane. For example, when the concentration of the drug is 50 μg/mL, it can cause wrinkles on the surface of some bacterial cell membranes (Figure 1B and 1D). However, when the drug concentration doubled to 100 μg/mL, most of the bacterial cells in the picture were seen to be destroyed, and only a small number of cells were irregular (Figure 1C and 1E). In contrast, when the concentration of the compound on plant bacteria is 0 μg/mL, the cells are plump and the surface is not wrinkled (Figure 1A and 1D). The pictures of these plant bacterial cells under different concentrations of the compound show that the compound destroys the cells with increasing concentration and eventually kills the cells.

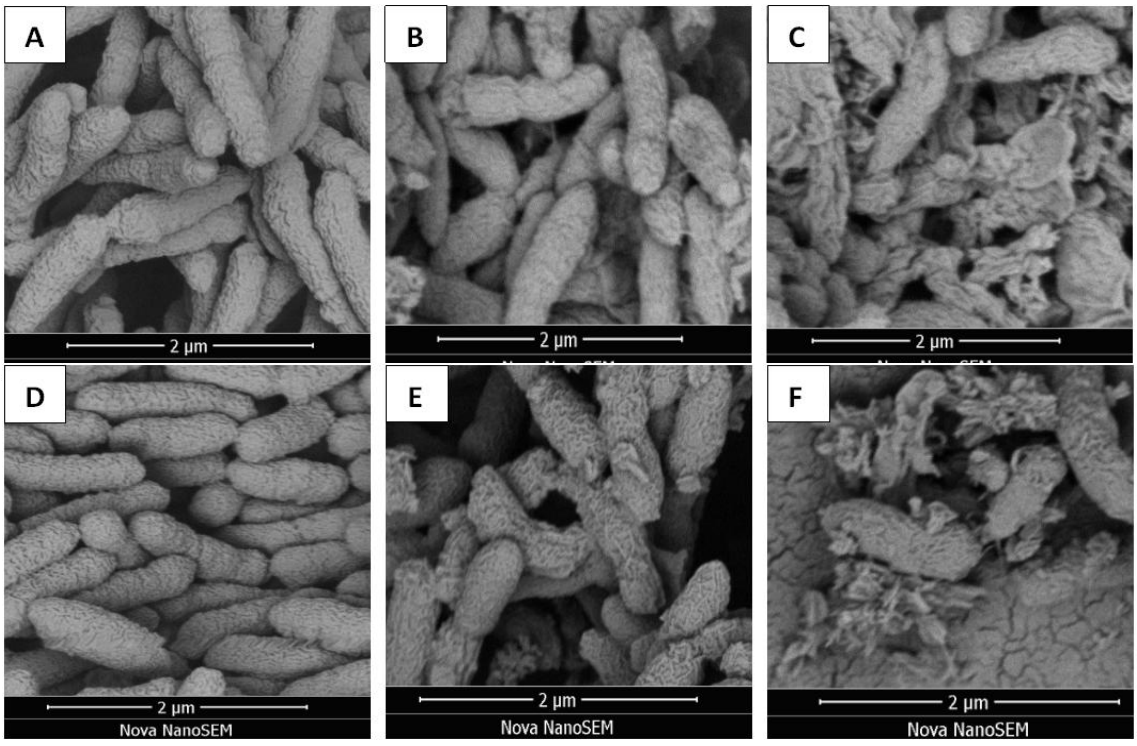

Figure 1. Scanning electron microscopy images for Xac and Xoo after incubated using different concentrations of compounds **3k**(Xac) and **3e**(Xoo), (A) 0 μg/mL, (B) 50 μg/mL and (C) 100 μg/mL, (D) 0 μg/mL, (E) 50 μg/mL and (F) 100 μg/mL. Scale bar for A、B、C、D、E、F are 2 μm.

Antiviral activity of target compounds against tobacco mosaic virus in vivo

The tobacco leaves of the same size and age were selected, and the in vivo treatment, protection and inactivation activity of 500 μg/mL tobacco mosaic virus was tested by the half leaf blob method. To this end, ningnanmycin, a commercially available and agricultural antiviral agent, was used as a

control agent. The preliminary antiviral bioassay results obtained are shown in Table 3. It can be seen from Table 3 that some compounds have good antiviral biological activity. Among them, compounds **3b, 3e, 3g, 3j, 3k, 3l, 3m** show excellent therapeutic activity against tobacco mosaic virus, with inhibition rates of 73.2 and 62.3%, respectively, 74.3, 61.4, 58.4, 55.2, 69.7%, which is better than the control drug ningnanmycin (53.3%). **3b, 3e, 3g, 3m** (70.1, 65.2, 70.6, and 68.1%, respectively) were more effective in protecting tobacco mosaic virus than the control drug ningnanmycin (62.6%). In particular, compounds **3h, 3j,** and **3m** showed excellent inactivation activity against tobacco mosaic virus, with inhibition rates of 83.2, 79.2, and 81.2%, which were superior to the control drug ningnanmycin (78.3%).

Table 3. Antiviral activities of the test compounds against tobacco mosaic virus in vivo at 500 μg/mL.

Compounds	R	Curative activity(%) [a]	Protective activity(%) [a]	Inactivation activity(%) [a]
3a	4-Cl-Ph	45.2±2.7	42.3±3.2	76.1 ± 2.4
3b	4-F-Ph	73.2±1.8	70.1±1.5	55.1 ±1.7
3c	2-Cl-Ph	37.0±1.1	35.2±3.8	68.2 ± 1.9
3d	4-CH_3-Ph	42.8±2.5	45.1±1.2	60.2 ± 1.1
3e	3-NO_2-Ph	62.3±1.7	65.2±1.1	77.2 ± 1.8
3f	4-OCH_3-Ph	47.2±1.3	37.8±3.3	68.1 ± 3.1
3g	4-NO_2-Ph	74.3±2.4	70.6±1.8	72.5 ± 0.9
3h	2-F-Ph	49.2±1.2	48.4±2.7	83.2 ± 2.9
3i	3-CH_3-Ph	28.2±1.9	31.4±3.2	68.1 ± 2.7
3j	3-Br-Ph	61.4±1.2	62.1±2.2	79.2 ± 1.4
3k	4-Br-Ph	58.4±2.1	49.8±2.1	65.3 ± 2.1
3l	2,4-di-Cl-Ph	55.2±2.5	50.1±1.9	68.1 ± 2.7
3m	4-C_3H_7-Ph	69.7±2.8	68.1±2.0	81.2 ± 0.8
3n	2-Thiophene	32.9±3.3	37.2±4.1	55.2 ± 4.2
3o	2-Furan	28.5±2.0	39.1±1.7	65.3 ± 3.3
Ningnanmycin [b]	-	53.3±1.2	62.6±1.3	78.3 ± 1.5

[a] Average of three replicates. [b] The commercial antiviral agent Ningnanmycin.

Structure-activity relationships of antiviral activities

The antiviral activity test showed that some chalcone malonate derivatives had significant biological activity against tobacco mosaic virus virus, which could be further analyzed and studied from different substituents of the compound. First, when the substituent R is 4-F-Ph、3-NO_2-Ph、4-NO_2-Ph、3-Br-Ph、4-Br-Ph、2,4-di-Cl-Ph、4-C_3H_7-Ph groups, the curative activity of the corresponding compounds **3b**、**3e**、**3g**、**3j**、**3k**、**3l**、**3m** on tobacco mosaic virus is significantly improved, which is better than ningnanmycin. When further studying the protective activity, it can be found that when the concentration of the compounds is 500 μg/mL and the substituent R is 4-F-Ph、3-NO_2-Ph、4-NO_2-Ph、4-C_3H_7-Ph groups, the protective activity of the compounds **3b**、**3e**、**3g**、**3m** is better than that of the other substituent compounds and the control antiviral agent. However, when comparing the inactivation activity, it can be clearly seen that the different effects of the substituents are small. When the substituent R is 2-F-Ph (**3h**)、3-Br-Ph (**3j**)、4-C_3H_7-Ph (**3m**) groups, the corresponding compounds is only slightly better than other compounds and ningnanmycin. The antiviral activity values of the compounds can be seen in Table 3.

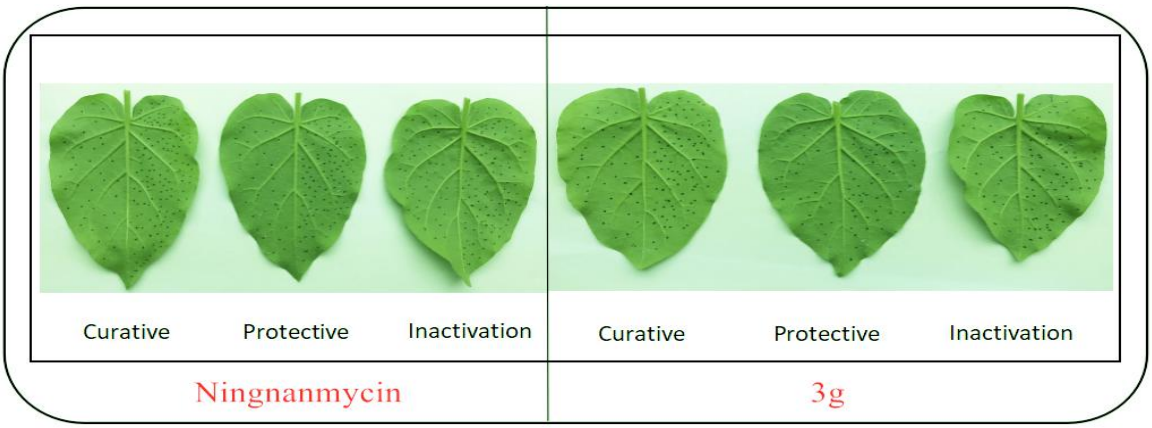

Figure 2. Tobacco leaf morphology effects of the ningnanmycin and **3g** against tobacco mosaic virus in vivo.(Right leaf: not treated with compound; Left leaf: smeared with compound).

*Binding sites of **3b**, **3g**, **3i** and ningnanmycin to tobacco mosaic virus-coat protein*

To further analyze the interactions between the target compounds and tobacco mosaic virus-coat protein (TMV-CP), the microscale thermophoresis (MST) analysis was used. The microscale thermophoresis results as summarized in Figure 3 show that the binding of compounds **3b**、**3g**、**3i**、ningnanmycin to tobacco mosaic virus-coat protein protein yielded Kd values of 0.211 ± 0.130 μmol/L、0.166 ± 0.077 μmol/L、80.867 ± 45.018 μmol/L、0.596 ± 0.338 μmol/L, respectively. As indicated in microscale thermophoresis, **3b** or **3g** with ningnanmycin share strong affinity, which is contrary to **3i** as it shares weak affinity. These results exhibited that the combining capacity in the following order of **3g** > **3b** > ningnanmycin > **3i** is consistent with the trends of the screening of antiviral activities. Based on the experimental results it can be predicted that compounds **3b** and **3g** may interact with tobacco mosaic virus-coat protein. As depicted in Figure 3 the bioactivity was mainly determined by the electrostatic interactions, and the activity could have been enhanced by the presence of aromatic ring which is rich in electrons for absorption. For example, when R was substituted with 4-F-Ph and 4-NO_2-Ph groups, the corresponding compounds **3b** and **3g** exhibited a stronger combining capacity, with Kd values of 0.211 ± 0.130 μmol/L and 0.166 ± 0.077 μmol/L, as compared to that of compound **3i** (80.867 ± 45.018 μmol/L), which was substituted with a 3-CH_3-Ph.

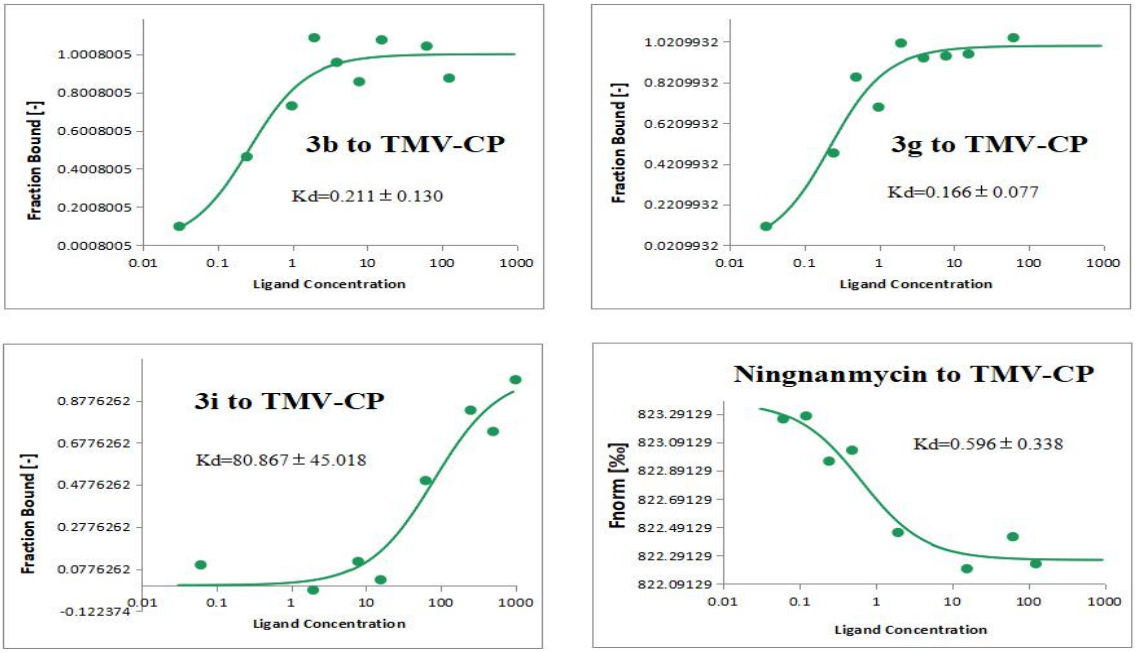

Figure 3. Microscale thermophoresis results of compounds **3b**, **3g**, **3i** and ningnamycin.

*Molecular docking of **3b** or **3g** and tobacco mosaic virus-coat protein*

To identify the **3b** and **3g** recognition sites in tobacco mosaic virus-coat protein (PDB code: 1EI7), we performed molecular docking using the Gold method with 200 cycles. As depicted in Figure 4, the two compounds were well-embedded in the activity pocket (ARG-46, THR-42, ARG-90, GLN-39, GLN-39, etc) between the two subunits of tobacco mosaic virus-coat protein. Among them, GLN-39 had strong hydrogen bond with **3b** (2.168 Å), C=O (**3b**) demonstrates two hydrogens with the ARG-46 (O-H=2.253 Å), ARG-90 (O-H=2.685 Å). Moreover, ARG-90 showed one hydrogen bond **3g** (1.834 Å), there was also one hydrogen bond between the C=O and the residue ARG-46 (O-H=1.993 Å) and THR-42 (O-H=2.205 Å). In addition, GLN-34 had strong hydrogen bond with ningnanmycin (1.798 Å), C=O (ningnanmycin) demonstrates one hydrogens with the ARG-90 (2.231 Å). It can be seen that the combination of **3b** and **3g** with tobacco mosaic virus-coat protein has several more stable hydrogen bonds than ningnanmycin and tobacco mosaic virus-coat protein, thus indicating that **3b** and **3g** have better antiviral activity than ningnanmycin. These interactions between molecules and tobacco mosaic virus-coat protein are likely to weaken the interaction of two subunits of tobacco mosaic virus-coat protein, thereby preventing the self-assembly of tobacco mosaic virus particle, as well as the binding capability with tobacco mosaic virus-coat protein. The results of molecular docking studies were consistent with the experimental results (protection and curative activities) and support that the chalcone derivatives containing malonate may be potential lead structures for developing novel anti-tobacco mosaic virus agents.

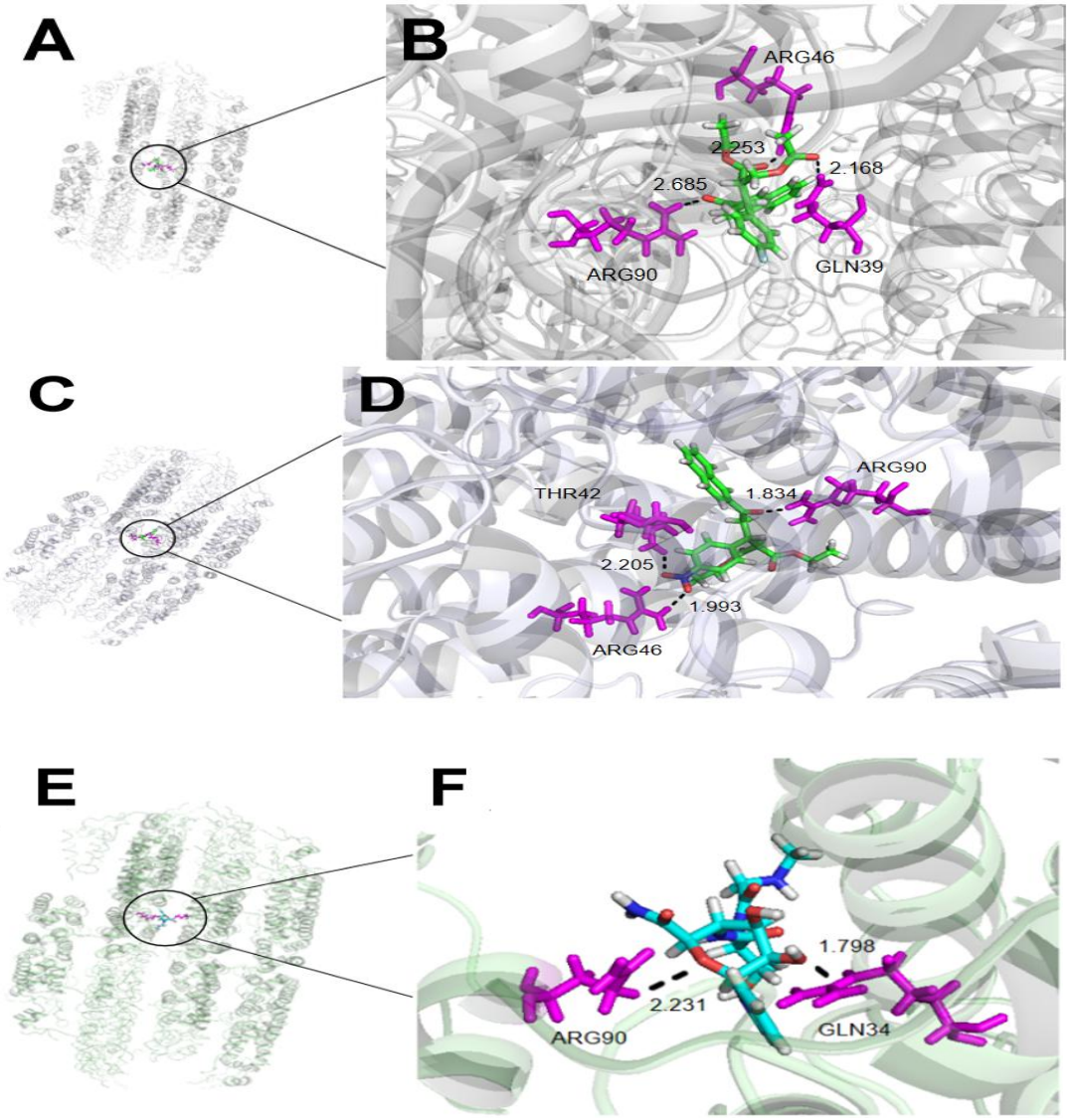

Figure 4. Molecular docking studies of compounds **3b** (A,B), **3g** (C,D) and ningnanmycin(E,F).

Conclusions

In this paper, malonate, chalcone and substituted benzaldehyde were used as raw materials to synthesize 15 chalcone derivatives containing malonate. The biological activity test proved that most of the compounds have a good inhibitory effect on Xoo, Xac, RS and tobacco mosaic virus. Among them, compound **3e** has a better inhibitory effect on Xoo than the control bactericide; compound 3b, 3g and 3m have better curative and protective activity against tobacco mosaic virus than the control drug ningnanmycin. Scanning electron microscopy images of compounds 3e and 3k indicate that the compound is potential Efficient fungicide. The microscale thermophoresis experiments of the compounds **3b**, **3g** and tobacco mosaic virus-coat protein showed that the binding force of these two compounds to tobacco mosaic virus-coat protein was better than that of ningnanmycin. The molecular docking study further confirmed that these small molecule compounds are compounds with excellent antiviral activity based on the experimental research of microscale thermophoresis. These action mechanisms have laid a foundation for studying the antibacterial and antiviral mechanism of chalcone derivatives. Although this study has a simple synthetic route, the compound has high biological activity. If it can become a commercial drug, it will save a lot of economic costs because of the simple synthesis step. In addition, the mechanism research has also been carried out in a systematic way, which can prove the high biological activity of this compound from many aspects.

Experimental Section

General

Bruker ASCEND 400 Nuclear Magnetic Resonance Spectrometer [400 MHz, Tetramethylsilane (TMS) as internal standard, DMSO as solvent, Bruker, Switzerland]. Thermo Scientific Q Exactive High Resolution Mass Spectrometer (HRMS, Thermo Fisher Scientific). Model XZ4 Digital Micrometer Melting Point Tester (Beijing Taike Instrument). Sartorius Electronic Balance (German Sartorius Group). Model 20 UV Analyzer (Shanghai Anting Electronic Instrument Factory). Substituted benzaldehyde was purchased from Shanghai Titan Technology. Malonate was purchased from Shanghai Nuote Biotechnology Co., Ltd., and other reagents were commercially available analytical grade. The molecular docking was performed by using DS-CDocker implemented in Discovery Studio (version 4.5).

Chemistry

*General procedure for the synthesis of **intermediate 1***

Reflux a mixture of an ethanol substrate (0.5 mmol), 1-(naphthalen-2-yl)ethan-1-ol (2 mmol), and tBuOK (4 mmol) in toluene (30 mL) with stirring under a nitrogen atmosphere in a system connected to a bubbler open to air for 14 h at 110 ° C. Cool the reaction mixture and condense under reduced pressure obtained **intermediate 1**, yellow solid, yield 62.2%.

*General procedure for the synthesis of **intermediate 2***

At first, Aqueous sodium hydroxide solution (20 % NaOH, 10 mmol) was added to a round-bottomed flask containing 1-(naphthalen-2-yl)ethan-1-one and differently substituted aldehydes (8 mmol). The mixture was stirred at ambient temperature for 12 h. TLC followed the progress of the reaction. After the reaction was completed, the reaction system was poured into ice water and acidified with hydrochloric acid. A solid precipitated and was filtered and dried to obtain **intermediate 2**, yellow solid, yield 53.5%..[38]

*General procedure for the synthesis of target compounds **3a-30***

A solution of **intermediate 2** (5 mmol), KOH (2mmol) and malonate (10 mmol) in methanol (50 mL) was stirred until dissolved, the reaction mixture was refluxed at 70 ℃ for 8 h. After completion of the reaction, the whole reaction system was poured into water, adjust pH to neutral, stirring with a glass rod to obtain a compounds, and the compounds was purified by column chromatography on silica gel with a mixture (V(petroleum ether):V(ethyl acetate) = 5:1) to yield the target compounds **3a-30**.[39]

diethyl 2-(1-(4-chlorophenyl)-3-(naphthalen-2-yl)-3-oxopropyl) malonate(**3a**): White solid, yield 56.2%, m.p. 98.3-99.7 °C; ^{1}H NMR (400 MHz, DMSO-d_6) δ 8.65 (s, 1H, Np-1-H), 8.12 (d, J = 7.8 Hz, 1H, Np-4-H), 8.00 (dd, J = 8.3, 3.8 Hz, 2H, Np-8,5-H), 7.93 (dd, J = 8.6, 1.7 Hz, 1H, Np-3-H), 7.71 - 7.61 (m, 2H, Np-6,7-H), 7.44 (d, J = 8.6 Hz, 2H, Ar(4-Cl)-3,5-H), 7.33 (d, J = 8.5 Hz, 2H, Ar(4-Cl)-2,6-H), 4.26 - 4.14 (m, 2H, Ar-CH-, CO_2-CH-), 4.10 - 4.05 (m, 2H, CO_2-CH_2-), 3.94 - 3.83 (m, 3H, CO_2-CH-, Ar-CH-CH_2-), 3.63 - 3.54 (m, 1H, CO-CH-), 1.19 (t, J = 7.1 Hz, 3H, CO_2-C-CH_3), 0.93 (t, J = 7.1 Hz, 3H, CO_2-C-CH_3); ^{13}C NMR (101 MHz, DMSO-d_6) δ 197.92, 168.23, 167.74, 140.18, 135.52, 134.19, 132.55, 131.94, 130.88, 130.30, 130.00, 129.15, 128.78, 128.45, 128.12, 127.44, 123.86, 61.85, 61.30, 57.12, 42.67, 14.29, 13.99. HRMS calcd for $C_{26}H_{25}ClO_5$ $[M + H]^+$ 453.1463, found 453.1461.

diethyl 2-(1-(4-fluorophenyl)-3-(naphthalen-2-yl)-3-oxopropyl)malonate(**3b**): Yellow oil, yield 61.8%; ^{1}H NMR (400 MHz, DMSO-d_6) δ 8.63 (s, 1H, Np-1-H), 8.10 (d, J = 7.8 Hz, 1H, Np-4-H), 7.99 (d, J = 8.6 Hz, 2H, Np-8,5-H), 7.90 (dd, J = 8.6, 1.5 Hz, 1H, Np-3-H), 7.71 - 7.58 (m, 3H, Np-7,6-H, Ar(4-F)-2-H), 7.36 (dd, J = 7.9, 1.1 Hz, 1H, Ar(4-F)-6-H), 7.25 (tt, J = 7.5, 3.7 Hz, 1H, Ar(4-F)-3-H), 7.21 - 7.14 (m, 1H, Ar(4-F)-5-H), 4.59 (td, J = 9.4, 4.8 Hz, 1H, Ar-CH-), 4.23 - 4.08 (m, 3H, CO_2-CH_2-, CO_2-CH-), 3.94 - 3.84 (m, 2H, CO_2-CH-, Ar-CH-CH-), 3.80 - 3.61 (m, 2H, Ar-CH-CH-, CO-CH-), 1.14 (t, J = 7.1 Hz, 3H, CO_2-C-CH_3), 0.90 (t, J = 7.1 Hz, 3H, CO_2-C-CH_3); ^{13}C NMR (101 MHz, DMSO-d_6) δ 197.71, 168.26, 167.58, 138.77, 135.51, 134.11, 134.02, 132.56, 130.35, 130.02, 129.85, 129.16, 128.82, 128.76, 128.14, 127.57, 127.46, 123.94, 61.86, 61.34, 56.26, 42.43, 36.96, 14.26, 13.95. HRMS calcd for $C_{26}H_{25}FO_5$ $[M + H]^+$ 437.1759, found 437.1751.

diethyl 2-(1-(2-chlorophenyl)-3-(naphthalen-2-yl)-3-oxopropyl)malonate(**3c**): White solid, yield 71.1%, m.p. 87.2-88.9 °C; ^{1}H NMR (400 MHz, DMSO-d_6) δ 8.64 (s, 1H, Np-1-H), 8.11 (d, J = 7.9 Hz, 1H, Np-4-H), 8.02 - 7.96 (m, 2H, Np-8,5-H), 7.94 - 7.88 (m, 1H, Np-3-H), 7.71 - 7.60 (m, 2H, Np-7-H, Ar(2-Cl)-3-H), 7.43 (dd, J = 8.6, 5.5 Hz, 2H, Np-6-H, Ar(2-Cl)-6-H), 7.09 (t, J = 8.9 Hz, 2H, Ar(2-Cl)-4,5-H), 4.25 - 4.13 (m, 2H, Ar-CH-, CO_2-CH-), 4.09 - 4.03 (m, 2H, CO_2-CH_2-), 3.93 - 3.81 (m, 3H, CO_2-CH-, Ar-CH-CH_2-), 3.60 - 3.49 (m, 1H, CO-CH-), 1.19 (t, J = 7.1 Hz, 3H, CO_2-C-CH_3), 0.91 (t, J = 7.1 Hz, 3H, CO_2-C-CH_3); ^{13}C NMR (101 MHz, DMSO-d_6) δ 197.71, 168.26, 167.58, 138.77, 135.51, 134.11, 134.02, 132.56, 130.35, 130.02, 129.85, 129.16, 128.82, 128.76, 128.14, 127.57, 127.46, 123.94, 61.86, 61.34, 56.26, 42.43, 36.96, 14.26, 13.95. HRMS calcd for $C_{26}H_{25}ClO_5$ $[M + H]^+$ 453.1463, found 453.1459.

diethyl 2-(3-(naphthalen-2-yl)-3-oxo-1-(p-tolyl) propyl) malonate(**3d**): White solid, yield 61.6%, m.p. 65.2-66.8 °C; ^{1}H NMR (400 MHz, DMSO-d_6) δ 8.64 (s, 1H, Np-1-H), 8.11 (d, J = 7.0 Hz, 1H, Np-4-H), 8.01 - 7.96 (m, 2H, Np-8,5-H), 7.91 (dd, J = 8.6, 1.6 Hz, 1H, Np-3-H), 7.70 - 7.60 (m, 2H, Np-7,6-H), 7.25 (d, J = 8.1 Hz, 2H, Ar(4-CH_3)-2,6-H), 7.04 (d, J = 7.9 Hz, 2H, Ar(4-CH_3)-3,5-H), 4.24 - 4.13 (m, 2H, Ar-CH-, CO_2-CH-), 4.03 (dt, J = 13.4, 7.1 Hz, 2H, CO_2-CH_2-), 3.91 - 3.77 (m, 3H, CO_2-CH-, Ar-CH-CH_2-), 3.56 - 3.47 (m, 1H, CO-CH-), 2.20 (s, 3H, CO_2-C-CH_3), 1.18 (t, J = 7.1 Hz, 3H, CO_2-C-CH_3), 0.91 (t, J = 7.1 Hz, 3H, CH_3); ^{13}C

NMR (101 MHz, DMSO-d_6) δ 198.07, 168.43, 167.81, 138.05, 136.26, 135.48, 134.32, 132.58, 130.26, 130.00, 129.10, 129.06, 128.75, 128.11, 127.41, 123.91, 61.74, 61.15, 57.51, 42.84, 40.80, 21.01, 14.30, 14.00. HRMS calcd for $C_{27}H_{28}O_5$ $[M + H]^+$ 433.2010, found 433.2006.

diethyl 2-(3-(naphthalen-2-yl)-1-(3-nitrophenyl)-3-oxopropyl)malonate(**3e**): Yellow solid, yield 55.4%, m.p. 96.2-97.3 °C; ^{1}H NMR (400 MHz, DMSO-d_6) δ 8.67 (s, 1H, Np-1-H), 8.36 (t, J = 1.9 Hz, 1H, Ar(4-NO_2)-2-H), 8.10 (ddd, J = 8.9, 8.2, 4.2 Hz, 2H, Np-4-H, Ar(4-NO_2)-4-H), 8.00 (dd, J = 8.3, 4.3 Hz, 2H, Np-8,5-H), 7.94 (dd, J = 8.7, 1.7 Hz, 2H, Np-3,7-H), 7.72 - 7.58 (m, 3H, Ar(4-NO_2)-6,5-H, Np-6-H), 4.27 - 4.17 (m, 4H, Ar-CH-, CO_2-CH_2-, CO_2-CH-), 4.08 - 3.98 (m, 1H, CO_2-CH-), 3.92 (q, J = 7.1 Hz, 2H, Ar-CH-CH_2-), 3.71 (dd, J = 13.7, 5.6 Hz, 1H, CO-CH-), 1.21 (t, J = 7.1 Hz, 3H, CO_2-C-CH_3), 0.92 (t, J = 7.1 Hz, 3H, CO_2-C-CH_3); ^{13}C NMR (101 MHz, DMSO-d_6) δ 197.83, 168.08, 167.73, 148.00, 143.64, 136.11, 135.55, 134.06, 132.53, 130.38, 130.04, 129.99, 129.19, 128.79, 128.12, 127.46, 123.82, 122.40, 61.97, 61.43, 56.67, 42.45, 40.73, 14.26, 13.96. HRMS calcd for $C_{26}H_{25}NO_7$ $[M + H]^+$ 464.1704, found 464.1699.

diethyl 2-(1-(4-methoxyphenyl)-3-(naphthalen-2-yl)-3-oxopropyl)malonate(**3f**): Yellow solid, yield 53.8%, m.p. 82.0-83.7 °C; ^{1}H NMR (400 MHz, DMSO-d_6) δ 8.64 (s, 1H, Np-1-H), 8.11 (t, J = 6.0 Hz, 1H, Np-4-H), 8.02 - 7.96 (m, 2H, Np-8,5-H), 7.95 - 7.90 (m, 1H, Np-3-H), 7.70 - 7.60 (m, 2H, Np-7,6-H,), 7.29 (d, J = 8.7 Hz, 2H, Ar(4-OCH_3)-2,6-H), 6.81 (d, J = 8.7 Hz, 2H, Ar(4-OCH_3)-3,5-H), 4.18 (qdd, J = 11.4, 7.6, 4.0 Hz, 2H, Ar-CH-, CO_2-CH-), 4.02 (dt, J = 14.4, 7.1 Hz, 2H, CO_2-CH_2-), 3.85 (ddd, J = 25.9, 15.5, 8.0 Hz, 3H, CO_2-CH-, Ar-CH-CH_2-), 3.67 (s, 3H, OCH_3), 3.54 - 3.47 (m, 1H, CO-CH-), 1.19 (t, J = 7.1 Hz, 3H, CO_2-C-CH_3), 0.92 (t, J = 7.1 Hz, 3H, CO_2-C-CH_3); ^{13}C NMR (101 MHz, DMSO-d_6) δ 198.15, 168.45, 167.85, 158.48, 135.48, 134.33, 132.87, 132.57, 130.26, 130.00, 129.96, 129.10, 128.74, 128.11, 127.41, 123.92, 113.84, 61.73, 61.14, 57.62, 55.32, 42.95, 14.31, 14.04. HRMS calcd for $C_{27}H_{28}O_6$ $[M + H]^+$ 449.1959, found 449.1953.

diethyl 2-(3-(naphthalen-2-yl)-1-(4-nitrophenyl)-3-oxopropyl)malonate(**3g**): White solid, yield 45.3%, m.p. 101.2-102.1 °C; ^{1}H NMR (400 MHz, DMSO-d_6) δ 8.64 (s, 1H, Np-1-H), 8.18 - 8.09 (m, 3H, Np-4-H, Ar(4-NO_2)-3,5-H), 8.00 (dd, J = 8.1, 3.6 Hz, 2H, Np-8,5-H), 7.91 (dd, J = 8.6, 1.5 Hz, 1H, Np-3-H), 7.74 - 7.62 (m, 4H, Np-6,7-H, Ar(4-NO_2)-2,6-H), 4.25 - 4.13 (m, 4H, Ar-CH-, CO_2-CH_2-, CO_2-CH-), 4.00 - 3.86 (m, 3H, CO_2-CH-, Ar-CH-CH_2-), 3.71 - 3.62 (m, 1H, CO-CH-), 1.19 (t, J = 7.1 Hz, 3H, CO_2-C-CH_3), 0.92 (t, J = 7.1 Hz, 3H, CO_2-C-CH_3); ^{13}C NMR (101 MHz, DMSO-d_6) δ 197.69, 168.02, 167.61, 149.43, 146.88, 135.56, 134.02, 132.53, 130.47, 130.35, 130.01, 129.23, 128.83, 128.14, 127.50, 123.81, 123.60, 62.01, 61.48, 56.66, 42.47, 14.28, 14.01. HRMS calcd for $C_{26}H_{25}NO_7$ $[M + H]^+$ 464.1704, found 464.1700.

diethyl 2-(1-(2-fluorophenyl)-3-(naphthalen-2-yl)-3-oxopropyl)malonate(**3h**): Yellow solid, yield 61.6%, m.p. 89.7-90.4 °C; ^{1}H NMR (400 MHz, DMSO-d_6) δ 8.64 (s, 1H, Np-1-H), 8.10 (t, J = 6.3 Hz, 1H, Np-4-H), 8.03 - 7.96 (m, 2H, Np-8,5-H), 7.94 - 7.88 (m, 1H, Np-3-H), 7.70 - 7.61 (m, 2H, Np-7-H, Ar(2-F)-4-H), 7.53 (t, J = 6.8 Hz, 1H, Np-6-H), 7.28 - 7.18 (m, 1H, Ar(2-F)-5-H), 7.14 - 7.06 (m, 2H, Ar(2-F)-2,3-H), 4.37 (td, J = 10.1, 4.1 Hz, 1H, Ar-CH-), 4.25 - 4.14 (m, 2H, CO_2-CH_2-), 4.07 (dd, J = 10.8, 5.3 Hz, 1H, CO_2-CH-), 3.92 - 3.77 (m, 3H, CO_2-CH-, Ar-CH-CH_2-), 3.61 (dd, J = 17.2, 3.9 Hz, 1H, CO-CH-), 1.18 (dt, J = 12.2, 6.3 Hz, 3H, CO_2-C-CH_3), 0.88 (dd, J = 12.6, 6.7 Hz, 3H, CO_2-C-CH_3); ^{13}C NMR (101 MHz, DMSO-d_6) δ 197.77, 168.19, 167.65, 162.02, 159.58, 135.52, 134.08, 132.56, 130.45, 130.41, 130.29, 130.02, 129.32, 129.24, 129.16, 128.78, 128.12, 128.01, 127.88, 127.44, 124.63, 124.60, 123.86, 115.81, 115.58, 61.91, 61.31, 56.31, 42.23, 34.33, 14.28, 13.91. ^{19}F NMR (376 MHz, DMSO-d_6) δ -116.00. HRMS calcd for $C_{26}H_{25}FO_5$ $[M + H]^+$ 437.1759, found 437.1757.

diethyl 2-(3-(naphthalen-2-yl)-3-oxo-1-(m-tolyl)propyl)malonate(**3i**): Yellow solid, yield 63.3%, m.p. 63.2-64.1 °C; ^{1}H NMR (400 MHz, DMSO-d_6) δ 8.63 (s, 1H, Np-1-H), 8.09 (t, J = 8.1 Hz, 1H, Np-4-H), 8.03 - 7.94 (m, 2H, Np-8,5-H), 7.93 - 7.87 (m, 1H, Np-3-H), 7.71 - 7.59 (m, 2H, Np-7,6-H), 7.19 - 7.07 (m, 3H, Ar(3-CH_3)-5,2,6-H), 6.95 (d, J = 7.0 Hz, 1H, Ar(3-CH_3)-4-H), 4.22 - 4.10 (m, 2H, Ar-CH-, CO_2-CH-), 4.04 - 3.96 (m, 2H, CO_2-CH_2-), 3.83 (ddd, J = 18.3, 15.3, 7.7 Hz, 3H, CO_2-CH-, Ar-CH-CH_2-), 3.50 (dd, J = 17.1, 2.8 Hz, 1H, CO-CH-), 2.23 (s, 3H, CH_3), 1.16 (t, J = 7.1 Hz, 3H, CO_2-C-CH_3), 0.88 (t, J = 7.1 Hz, 3H, CO_2-C-CH_3); ^{13}C NMR (101 MHz, DMSO-d_6) δ 198.07, 168.40, 167.81, 141.06, 137.42, 135.48, 134.30, 132.57, 130.31, 130.00, 129.60, 129.13, 128.74, 128.39, 128.12, 127.90, 127.44, 125.87, 123.91, 61.75, 61.14, 57.45, 42.77, 41.07, 21.45, 14.30, 13.99. HRMS calcd for $C_{27}H_{28}O_5$ $[M + H]^+$ 433.2010, found 433.2007.

diethyl 2-(1-(3-bromophenyl)-3-(naphthalen-2-yl)-3-oxopropyl)malonate(**3j**): Yellow oil, yield 64%; ^{1}H NMR (400 MHz, DMSO-d_6) δ 8.64 (s, 1H, Np-1-H), 8.11 (d, J = 7.9 Hz, 1H, Np-4-H), 8.03 - 7.96 (m, 2H, Np-8,5-H), 7.91 (dd, J = 8.6, 1.6 Hz, 1H, Np-3-H), 7.71 - 7.61 (m, 3H, Np-7,6-H, Ar(3-Br)-2-H), 7.42 - 7.34 (m, 2H, Ar(3-Br)-4,5-H), 7.21 (t, J = 7.8 Hz, 1H, Ar(3-Br)-6-H), 4.23 - 4.12 (m, 2H, Ar-CH-, CO_2-CH-), 4.04 (ddd, J = 14.2, 13.5, 7.1 Hz, 2H, CO_2-CH_2-), 3.93 - 3.83 (m, 3H, CO-CH-, Ar-CH-CH_2-), 3.56 (dd, J = 17.3, 3.6 Hz, 1H, CO-CH-), 1.18 (t, J = 7.1 Hz, 3H, CO_2-C-CH_3), 0.91 (t, J = 7.1 Hz, 3H, CO_2-C-CH_3); ^{13}C NMR (101 MHz, DMSO-d_6) δ 197.92, 168.17, 167.73, 143.97, 135.53, 134.16, 132.55, 131.77, 130.63, 130.36, 130.23, 130.01, 129.18, 128.79, 128.19, 128.14, 127.47, 123.86, 121.82, 61.88, 61.31, 56.99, 42.55, 40.85, 14.29, 14.01. HRMS calcd for $C_{26}H_{25}BrO_5$ $[M + H]^+$ 497.0958, found 497.0953.

diethyl 2-(1-(4-bromophenyl)-3-(naphthalen-2-yl)-3-oxopropyl)malonate(**3k**): White solid, yield 52.1%, m.p. 80.2-81.5 °C; ^{1}H NMR (400 MHz, DMSO-d_6) δ 8.63 (s, 1H, Np-1-H), 8.11 (d, J = 7.9 Hz, 1H, Np-4-H), 8.03 - 7.96 (m, 2H, Np-8,5-H), 7.91 (dd, J = 8.7, 1.2 Hz, 1H, Np-3-H), 7.71 - 7.60 (m, 2H, Ar(4-Br)-3,5-H), 7.45 (d, J = 8.4 Hz, 2H, Np-7,6-H), 7.36 (d, J = 8.4 Hz, 2H, Ar(4-Br)-2,6-H), 4.25 - 4.13 (m, 2H, Ar-CH-, CO_2-CH-), 4.09 - 4.02 (m, 2H, CO_2-CH_2-), 3.94 - 3.80 (m, 3H, CO_2-CH-, Ar-CH-CH_2-), 3.61 - 3.51 (m, 1H, CO-CH-), 1.18 (t, J = 7.1 Hz, 3H, CO_2-C-CH_3), 0.92 (t, J = 7.1 Hz, 3H, CO_2-C-CH_3); ^{13}C NMR (101 MHz, DMSO-d_6)

δ 197.92, 168.21, 167.73, 140.62, 135.53, 134.18, 132.55, 131.38, 131.25, 130.30, 130.01, 129.17, 128.80, 128.13, 127.47, 123.86, 120.46, 61.86, 61.31, 57.05, 42.61, 14.30, 14.00. HRMS calcd for $C_{26}H_{25}BrO_5$ $[M + H]^+$ 497.0958, found 497.0954.

diethyl 2-(1-(2,6-dichlorophenyl)-3-(naphthalen-2-yl)-3-oxopropyl)malonate(**3l**): Yellow solid, yield 47.9%, m.p. 98.2-99.3 °C; ^{1}H NMR (400 MHz, DMSO-*d*$_6$) *δ* 8.68 (s, 1H, Np-1-H), 8.11 (d, *J* = 7.8 Hz, 1H, Np-4-H), 8.00 (dd, *J* = 8.1, 4.3 Hz, 2H, Np-8,5-H), 7.94 (dd, *J* = 8.6, 1.5 Hz, 1H, Np-3-H), 7.71 - 7.60 (m, 2H, Np-7,6-H), 7.45 - 7.35 (m, 2H, Ar(2,6-di-Cl)-3,5-H), 7.24 (t, *J* = 8.0 Hz, 1H, Ar(2,6-di-Cl)-4-H), 5.08 (ddd, *J* = 11.6, 9.4, 4.5 Hz, 1H, Ar-CH-), 4.52 (d, *J* = 11.6 Hz, 1H, CO_2-CH-), 4.29 - 4.13 (m, 2H, CO_2-CH_2-), 4.02 (dd, *J* = 16.9, 9.4 Hz, 1H, CO_2-CH-), 3.82 (qdd, *J* = 16.9, 9.1, 5.8 Hz, 3H, Ar-CH-CH_2-, CO-CH-), 1.20 (t, *J* = 7.1 Hz, 3H, CO_2-C-CH_3), 0.85 (t, *J* = 7.1 Hz, 3H, CO_2-C-CH_3); ^{13}C NMR (101 MHz, DMSO-*d*$_6$) *δ* 197.57, 168.13, 167.21, 137.49, 135.53, 135.31, 135.00, 133.90, 132.58, 130.42, 130.38, 130.04, 130.01, 129.27, 129.15, 128.79, 128.12, 127.42, 123.97, 62.09, 61.35, 54.01, 36.96, 14.28, 13.82. HRMS calcd for $C_{26}H_{24}Cl_2O_5$ $[M + H]^+$ 487.1074, found 487.1070.

diethyl 2-(1-(4-isopropylphenyl)-3-(naphthalen-2-yl)-3-oxopropyl)malonate(**3m**): White solid, yield 70.2%, m.p. 74.2-75.7 °C; ^{1}H NMR (400 MHz, DMSO-*d*$_6$) *δ* 8.61 (d, *J* = 4.6 Hz, 1H, Np-1-H), 8.05 (d, *J* = 21.1 Hz, 1H, Np-4-H), 7.91 (dd, *J* = 19.7, 13.0 Hz, 3H, Np-8,5,3-H), 7.62 (dd, *J* = 15.7, 7.8 Hz, 2H, Np-7,6-H), 7.16 (d, *J* = 71.1 Hz, 4H, Ar(4-C_3H_7)-2,3,5,6-H), 4.14 (d, *J* = 6.2 Hz, 2H, Ar-CH-, CO_2-CH-), 3.98 (dd, *J* = 15.8, 9.9 Hz, 2H, CO_2-CH_2-), 3.82 (d, *J* = 5.6 Hz, 3H, CO_2-CH-, Ar-CH-CH_2-), 3.49 (d, *J* = 17.1 Hz, 1H, CO-CH-), 2.82 - 2.68 (m, 1H, -CH=), 1.18 - 1.12 (m, 3H, CO_2-C-CH_3), 1.08 (s, 6H, CO_2-C-CH_3, CH_3), 0.80 (d, *J* = 6.6 Hz, 3H, CH_3); ^{13}C NMR (101 MHz, DMSO-*d*$_6$) *δ* 198.06, 168.42, 167.94, 147.21, 138.42, 135.48, 134.27, 132.57, 130.30, 130.00, 129.10, 128.80, 128.72, 128.10, 127.40, 126.35, 123.90, 61.71, 61.08, 57.45, 42.84, 40.80, 33.43, 24.21, 14.29, 13.89. HRMS calcd for $C_{29}H_{32}O_5$ $[M + H]^+$ 461.2323, found 461.2318.

diethyl 2-(3-(naphthalen-2-yl)-3-oxo-1-(thiophen-2-yl)propyl)malonate(**3n**): Brown oil, yield 60%; ^{1}H NMR (400 MHz, DMSO-*d*$_6$) *δ* 8.67 (s, 1H, Np-1-H), 8.13 (d, *J* = 8.4 Hz, 1H, Np-4-H), 8.00 (dd, *J* = 8.6, 5.5 Hz, 2H, Np-8,5-H), 7.94 (dd, *J* = 8.6, 1.6 Hz, 1H, Np-3-H), 7.66 (dtd, *J* = 14.7, 7.0, 1.3 Hz, 2H, Np-7,6-H), 7.31 (dd, *J* = 5.1, 1.0 Hz, 1H, Th-3-H), 7.04 (d, *J* = 2.9 Hz, 1H, Th-4-H), 6.92 - 6.87 (m, 1H, Th-5-H), 4.39 (td, *J* = 9.5, 4.0 Hz, 1H, Th-CH-), 4.23 - 4.11 (m, 2H, CO_2-CH_2-), 4.06 - 3.95 (m, 3H, CO_2-CH_2-, Th-CH-CH-), 3.87 (dd, *J* = 17.4, 9.5 Hz, 1H, Th-CH-CH-), 3.57 (dt, *J* = 17.3, 4.7 Hz, 1H, CO-CH-), 1.20 - 1.15 (m, 3H, CO_2-C-CH_3), 1.02 (t, *J* = 7.1 Hz, 3H, CO_2-C-CH_3); ^{13}C NMR (101 MHz, DMSO-*d*$_6$) *δ* 197.70, 168.04, 167.67, 143.87, 135.55, 134.18, 132.59, 130.36, 130.06, 129.20, 128.82, 128.13, 127.47, 127.04, 126.11, 124.92, 123.89, 61.84, 61.46, 57.90, 43.51, 36.00, 14.29, 14.12. HRMS calcd for $C_{24}H_{24}O_5S$ $[M + H]^+$ 425.1417, found 425.1413.

diethyl 2-(1-(furan-2-yl)-3-(naphthalen-2-yl)-3-oxopropyl)malonate(**3o**): Brown oil, yield 53%; ^{1}H NMR (400 MHz, DMSO-*d*$_6$) *δ* 8.68 (s, 1H, Np-1-H), 8.14 (t, *J* = 7.2 Hz, 1H, Np-4-H), 8.01 (t, *J* = 8.0 Hz, 2H, Np-8,5-H), 7.96 (dd, *J* = 8.7, 1.7 Hz, 1H, Np-3-H), 7.69 - 7.66 (m, 1H, Np-7-H), 7.66 - 7.63 (m, 1H, Np-6-H), 7.52 - 7.49 (m, 1H, Fu-3-H), 6.31 (dd, *J* = 3.2, 1.9 Hz, 1H, Fu-4-H), 6.21 (d, *J* = 3.2 Hz, 1H, Fu-5-H), 4.27 - 4.10 (m, 3H, Fu-CH-, CO_2-CH_2-), 4.08 - 3.99 (m, 2H, CO_2-CH_2-), 3.98 - 3.94 (m, 1H, Fu-CH-CH-), 3.81 (dd, *J* = 17.4, 9.2 Hz, 1H, Fu-CH-CH-), 3.57 - 3.48 (m, 1H, CO-CH-), 1.16 (t, *J* = 7.1 Hz, 3H, CO_2-C-CH_3), 1.08 (t, *J* = 7.1 Hz, 3H, CO_2-C-CH_3); ^{13}C NMR (101 MHz, DMSO-*d*$_6$) *δ* 197.68, 167.99, 167.81, 154.20, 142.36, 135.57, 134.06, 132.61, 130.37, 130.09, 129.20, 128.82, 128.13, 127.46, 123.88, 110.78, 107.16, 61.76, 61.54, 55.46, 34.40, 14.28, 14.21. HRMS calcd for $C_{24}H_{24}O_6$ $[M + H]^+$ 409.1646, found 409.1640.

Antibacterial Bioassays

The turbidity method was used to test the target compounds with Xac, Xac, Rs using commercial bismerthiazol and thiodiazole copper as positive control agents.[40-42] Prepare a sterile nutrient broth culture medium: 3.0 g beef extract, 5.0 g peptone , 1.0 g of yeast powder, 10.0 g of glucose and 1000 mL of secondary water, pH 7.0 - 7.2. In a test tube, the test compound and the control agent are formulated into a 100 μg/mL and 50 μg/mL concentration medium and tested for OD. Value, the value is sterileThe OD value of the culture medium. 40 μL of the broth containing the bacteria was added to the sterile medium, and the inoculated test tube was continuously shaken at 28 rpm and 180 rpm for 36 to 48 hours, and then the OD value was measured. Calculate the inhibition rate by the following formula: Inhibition rate = (OD value of the bacterial solution of the control medium after correction-OD value of the toxic medium after correction) / OD value of the control medium bacterial solution after correction. Corrected OD value = OD value of bacteria-containing medium-OD value of sterile medium.

Antiviral Bioassays

Curative activity of the target compounds against tobacco mosaic virus in vivo

Take a heart leaf tobacco, trim it to keep 3 to 5 tobacco leaves, sprinkle emery sand evenly on each leaf, use a pen to dip tobacco mosaic virus virus (500 μg/mL), and brush it evenly on the tobacco leaves. Wait for the virus Inoculate the tobacco leaves (0.5 - 1 h), wash away the emery with water, and dry naturally. Use a writing brush to dip the target compound solvent (500 mg/mL) and apply evenly on the right half of the tobacco leaves. Move to 28 ℃ for humidification. After 2 to 3 days, obvious spots appear on the leaves, record the number of spots on the left and right sides, and bring them into the formula to calculate the inhibition rate. Each compound is performed 2 to 3 times in parallel.[43-45]

Protection activity of the target compounds against tobacco mosaic virus in vivo

Take a heart leaf tobacco, trim it to retain 3 to 5 tobacco leaves, use a brush to dip the target compound solvent (500 mg/mL) and apply it evenly on the right half of the tobacco leaves. After 12 hours, sprinkle emery Dip the left and right sides of the leaf with tobacco mosaic virus virus (500 μg / mL), and brush it evenly on the tobacco leaf. After the virus is inoculated on the tobacco leaf (0.5 - 1 h), wash the emery with water to dry it. Moisturize and cultivate at 28 ℃. After 2 to 3 days, obvious spots appear on the leaves, record the number of spots on the left and right sides, and bring in the formula to calculate the inhibition rate. Each compound is performed 2 to 3 times in parallel. The inhibitory rate (I %) of the compound was calculated according to the following formula: (I %)= (Cnum – Tnum)/ Cnum× 100%. (Cnum: average local lesion number of control(not treated with compounds); Tnum: average local lesion number smeared with drugs.)

Inactivation activity of the target compounds against tobacco mosaic virus in vivo

The virus is initially added to the virus for 30 minutes. Take a heart leaf tobacco, trim it to retain 3 to 5 tobacco leaves, sprinkle evenly on each leaf, and use a pen to dip the virus after the action of the drug to spread evenly on the left half of the tobacco leaves. Use a row Dip the pen with tobacco mosaic virus virus (500 μg/mL) and brush it evenly on the right half of the leaf. After the virus is inoculated into tobacco leaves (0.5 - 1 h), wash away the emery with water, dry naturally, and move to 28 ℃ Cultivate. After 2 to 3 days, obvious spots appear on the leaves, record the number of spots on the left and right sides, and bring into the formula to calculate the inhibition rate. Each compound is performed 2 to 3 times in parallel. The inhibition rates (I %) of the compounds were calculated according to the following formula: (I %) = (Cnum – Tnum)/ Cnum× 100%. (Cnum: average local lesion number of control(not treated with compounds); Tnum: average local lesion number smeared with compounds.)

Scanning electron microscopy (SEM) study

Measure 1.5 mL of the germ solution that has grown to the logarithmic phase in a 2 mL centrifuge tube, centrifuge at low speed (6000 r / min) for about 1 minute, centrifuge the bacteria, and add 1 mL of PBS (pH = 7.2) to wash away. Medium, then add 1.5 mL of PBS buffer solution, gently resuspend with a pipette tip, and finally add the target compound solution to a concentration of 100 and 50 μg/mL, and blank control with dimethyl sulfoxide (DMSO) 10 μL, incubate at room temperature for 8-10 hours.

Pipette 1 mL of the bacterial solution after incubation in a 2 mL centrifuge tube at low speed (6000 r/min) for about 1 minute to centrifuge the bacteria into pellets, discard the supernatant, and wash the precipitated cells with 1 mL of PBS solution 3 times to wash Remove the drug; add 1 mL of 2.5% glutaraldehyde fixative for 8-10 hours or overnight (4 ℃), discard the fixation solution, and wash 3 times with 1 mL of PBS solution to wash off the glutaraldehyde; 1 mL of 30%, 50%, 70%, 90%, 100% (three times) ethanol was sequentially dehydrated and replaced (about 10-15 minutes each time), and the dehydrated samples were placed in a freeze dryer and freeze-dried for 2 h; dried The bacterial cell powder was subjected to scanning electron microscopy testing after sticking samples and spraying gold.[46]

Interaction studies between 3b, 3g, 3i and ningnanmycin with tobacco mosaic virus-coat protein

Take 75 μL of purified tobacco mosaic virus-coat protein,[47] and incubate for 30 min in the dark; load the labeled protein into the elution column, elute with phosphate buffer saline (PBS) and collect the protein. Add 10 μL of gradient dilution (500, 250, 125, 62.5, 31.25, 15.625, 7.813, 3.906, 1.953, 0.977, 0.488, 0.244, 0.122, 0.061, 0.0305, 0.01525 μmol/L) of compound 3b to each PCR tube. Then, mix 10 μL of the labeled protein and 10 μL of the diluted molecules, and after 5 min incubation, load each tube of the complex into a capillary pipette, then place it on the capillary pipette tray and measure with an instrument. Tobacco mosaic virus-coat protein is obtained in the previous work of the research group.

Molecular Docking study

Molecule docking study were obtained by using DS-CDoking implemented in Discovery Studio (version 4.5).[45] First, the target protein molecule PDB file was obtained, which can be searched from the PDB database website. Acquire PDB or mol2 files of small molecules at the same time. The Dock program requires that the molecular file has a mol2 structure, because the mol2 file can record the generation amount of each atom in the molecule, etc., and contains more information. When preparing a molecular docking file, first process the target protein molecule, remove other small molecules and water molecules contained in the target protein PDB file, and then do the same for the small molecule to be docked, hydrogenate, and save it in Mol2 format.

Supplementary Material

Supporting information for this article is available on the WWW under http://dx.doi.org/10.1002/MS-number.

Acknowledgements

This research was supported by the National Key Research and Development Program of China (No.2018YFD02011026), the Science and Technology Project of Guizhou Province (Nos. 20192452, 20191105) and the Graduate Education Innovation Program of Guizhou Province (YJSCXJH2019018).

Author Contribution Statement

The current study is an outcome of constructive discussion with Wei Xue and Tao Guo, who carried out synthesis and characterization experiments; Tao Guo, Rongjiao Xia and Tingting Liu performed the antiviral and antibacterial activity determination; Feng Peng, Xuemei Tang and Qing Zhou carried out the ^{1}H NMR, ^{13}C NMR, ^{19}F NMR and HRMS spectral analyses;Hui Luo scanned the electron microscope.

References

[1] Q. L. Dang, W. K. Kim, C. M. Nguyen, Y. H. Choi, G. J. Choi, K. S. Jang, C. H. Lim, N. H. Luu, J. C. Kim, 'Nematicidal and Antifungal Activities of Annonaceous Acetogenins from Annona squamosa against Various Plant Pathogens', *J. Agric. Food Chem*. **2011**, *59*, 11160–11167.

[2] D. F. Lorenzo, A. Palmigiano, A. Silipo, Y. Desaki, D. Garozzo, R. Lanzetta, N. Shibuya, A. Molinaro, 'The structure of the lipooligosaccharide from Xanthomonas oryzae pv. Oryzae: the causal agent of the bacterial leaf blight in rice', *Carbohyd. Res*. **2016**, *427*, 38–43.

[3] B. Li, B. P. Liu, C. L. Shan, M. Ibrahim, Y. S. Lou, Y. L. Wang, G. L. Xie, H. Y. Li, G. H. Sun, 'Antibacterial activity of two chitosan solutions and their effect on rice bacterial leaf blight and leaf streak', *Pest. Manage. Sci*. **2013**, *69*, 312–320.

[4] D. Q. Pham, D. T. Ba, N. T. Dao, G. J. Choi, T. T. Vu, J. C. Kim, T. P. L. Giang, H. D. Vu, Q. Dang, 'Antimicrobial efficacy of extracts and constituents fractionated from Rheum tanguticum Maxim. ex Balf. rhizomes against phytopathogenic fungi and bacteria', *Ind. Crops Prod*. **2017**, *108*, 442–450.

[5] Y. Liang, D. S. Yang, J. H. Cui, 'A graphene oxide/silver nanoparticle composite as a novel agricultural antibacterial agent against Xanthomonas oryzae pv. oryzae for crop disease management', *New J. Chem*. **2017**, *41*, 13692–13699.

[6] B .Wang, G. C. Wu, Y. Q. Zhang, G. L. Qian, F. Q. Liu, 'Dissecting the virulence related functionality and cellular transcription mechanism of a conserved hypothetical protein in Xanthomonas oryzae pv. oryzae. Mol', *Plant Pathol*. **2018**, *19*, 1859–1872.

[7] A. Yugander, R. M. Sundaram, D. Ladhalakshmi, S. K. Hajira, V. Prakasam, M. S. Prasad, M. S. Madhav, V. R. Babu, G. S. Laha, 'Virulence profiling of Xanthomonas oryzae pv. oryzae isolates, causing bacterial blight of rice in India', *Eur. J. Plant Pathol*. **2017**, *149*, 171–191.

[8] H. P. T. Ngo, T. H. Ho, I. Lee, H. T. Tran, B. Sur, S. Kim,J. G. Kim, Y. J. Ahn,S. S. Cha, L. W. Kang, 'Crystal Structures of Peptide Deformylase from Rice Pathogen Xanthomonas oryzae pv. oryzae in Complex with Substrate Peptides, Actinonin, and Fragment Chemical Compounds', *J. Agric. Food Chem*. **2016**, *64*, 7307–7314.

[9] P. Y. Wang, L. Zhou, J. Zhou, Z. B. Wu, W. Xue, B. A. Song, S. Yang, 'Synthesis and antibacterial activity of pyridinium-tailored 2,5- substituted-1,3,4-oxadiazole thioether/sulfoxide/sulfone derivatives', *Bioorg. Med. Chem. Lett*. **2016**, *26*, 1214–1217.

[10] T. R. Gottwald , X. Sun, T. Riley, J. H. Graham, F. Ferrandino, E. L. Taylor, 'Geo-Referenced Spatiotemporal Analysis of the Urban Citrus Canker Epidemic in Florida', *Phytopathology*. **2002**, *92* , 361-377.

[11] C. M. Ference, A. M. Gochez, F. Behlau, N. Wang, J. H. Graham, J. B. Jones, 'Recent advances in the understanding of Xanthomonas citri ssp citri pathogenesis and citrus canker disease management', *Mol. Plant Pathol*. **2018**, *19*, 1302–1318.

[12] H. Mirzaei-Najafgholi, S. Tarighi, M. Golmohammadi, P. Taheri, 'The Effect of Citrus Essential Oils and Their Constituents on Growth of Xanthomonas citri subsp citri', *Molecules*. **2017**, *22*, 591-605.

[13] B. Su, C. L. Cai, M. Deng, Q. M. Wang, 'Spatial Configuration and Three-Dimensional Conformation Directed Design, Synthesis, Antiviral Activity, and Structure-Activity Relationships of Phenanthroindolizidine Analogues', *J. Agric. Food Chem*. **2016**, *64*, 2039-2045.

[14] R. J. Xia, T. Guo, M. Chen, S. J. Su, J. He, X. Tang, S. C. Jiang, W. Xue, 'Synthesis, antiviral and antibacterial activities and action mechanism of penta-1,4-dien-3-one oxime ether derivatives containing a quinoxaline moiety', *New J. Chem*. **2019**, *43*, 16461–16467.

[15] X. H. Gan, D. Y. Hu, P. Li, J. Wu, X. W. Chen, W. Xue, B. A. Song, 'Design, synthesis, antiviral activity andthree-dimensional quantitative structure-activity relationship study of novel 1,4-pentadien-3-one derivativescontaining the 1,3,4-oxadiazole moiety', *Pest. Manag. Sci*. **2016**, *72*, 534–543.

[16] T. Guo, R. J. Xia, M. Chen, J. He, S. J. Su, L. W. Liu, X. Y. Li, W. Xue, W, 'Biological activity evaluation and action mechanism of chalcone derivatives containing thiophene sulfonate', *RSC Advances*. **2019**, *9*, 24942–24950.

[17] X. M. Zhong, X. B. Wang, L. J. Chen,W. Xue, W, 'Synthesis and biological activity of myricetin derivatives containing 1,3,4-thiadiazole scaffold', *Chem. Cent. J*. **2017**, *11*, 106.

[18] S. Perumalsamy, M. Bharani, M. Sudha, P. Nagarajan, L. Arul, R. Saraswathi, P. Balasubramanian, J. Ramalingam, 'Functional marker-assisted selection for bacterial leaf blight resistance genes in rice (Oryza sativa L.)', *Plant. Breed*. **2010**, *129*, 400–406.

[19] Y. Q. Hu, S. Zhang,Z. Xu, Z. S. Lv, M. L. Liu, L. S. Feng, '4-Quinolone hybrids and their antibacterial activities', *Eur. J. Med. Chem*. **2017**, *141*, 335–345.

[20] Y. J. Lin, Z. L. He, E. N. Rosskopf, K. L. Conn,C. A. Powell, G. Lazarovits, 'A nylon membrane bag assay fordetermination of the effect of chemicals on soilborne plant pathogens in soil', *Plant. Dis*. **2010**, *94*, 201–206.

[21] R. Schobert, B. Biersack, A. Dietrich, 'Pt(II) Complexes of a Combretastatin A-4 Analogous Chalcone: Effects of Conjugation on Cytotoxicity, Tumor Specificity, and Long-Term Tumor Growth Suppression', *J. Med. Chem*. **2009**, *52*, 241–246.

[22] S. Vogel, M. Barbic, J. Guido, 'Synthesis, cytotoxicity, anti-oxidative and anti-inflammatory activity of chalcones and influence of A-ring modifications on the pharmacological effect', *Eur. J. Med. Chem*. **2010**, *45*, 2206–2213.

[23] V. Tomar, G. Bhattacharjee, 'Synthesis of new chalcone derivatives containing acridinyl moiety with potential antimalarial activity', *Eur. J. Med. Chem*. **2010**, *45*, 745–751.

[24] P. L. Zhao, C. L. Liu,W. Huang, Y. Z. Wang, G. F. Yang, 'Synthesis and Fungicidal Evaluation of Novel Chalcone-Based Strobilurin Analogues', *J. Agric. Food Chem*. **2007**, *55*, 5697–5700.

[25] R. Sribalan,G. Banuppriya, M. Kirubavathi, A. Jayachitra, G. Padmini, 'Multiple biological activities and molecular docking studies of newly synthesized 3-(pyridin-4-yl)-1H-pyrazole-5-carboxamide chalcone hybrids', *Bioorg. Med. Chem. Lett*. **2016**, *26*, 5624–5630.

[26] G. Pasquale,G. P. Romanelli, J. C. Autino, J. García, P. R. Duchowicz, 'Quantitative Structure–Activity Relationships of Mosquito Larvicidal Chalcone Derivatives', *J. Agric. Food Chem*. **2012**, *60*, 692–697.

[27] S. Attar, Z. O'Brien, H. Alhaddad, M. L.Golden,A. G. Urrea, 'Ferrocenyl chalcones versus organic chalcones: A comparative study of their nematocidal activity', *Bioorg. Med. Chem*. **2011**, *19*, 2055–2073.

[28] D. Coskun, M. Erkisa, E. Ulukaya, M. F. Coskun, F. Ari, 'Novel 1-(7-ethoxy-1-benzofuran-2-yl) substituted chalcone derivatives: Synthesis, characterization and anticancer activity', *Eur. J. Med. Chem*. **2017**, *136*, 212–222.

[29] X. H. Gan, D. Y. Hu, Y. J. Wang, L. Yu, B. A. Song, 'Novel trans-Ferulic Acid Derivatives Containing a Chalcone Moiety as Potential Activator for Plant Resistance Induction', *J. Agric. Food Chem*. **2017**, *65*, 4367–4377.

[30] A. L. Cole, S. Hossain, A. M. Cole, 'Synthesis and bioevaluation of substituted chalcones, coumaranones and other flavonoids as anti-HIV agents', *Bioorg. Med. Chem*. **2016**, *24*, 2768–2776.

[31] J. F. Li, D. Li, Y. M. Xu, Z. B. Guo, X. Liu, H. Yang, L. C. Wu, L. S. Wang, 'Design, synthesis, biological evaluation, and molecular docking of chalcone derivatives as anti-inflammatory agents', *Bioorg. Med. Chem. Lett*. **2017**, *27*, 602–606.

[32] Y. Z. Guo, H. Serrano, G. J. Poelarends, W. H. Johnson, M. L. Hackert, C. P. Whitman, Kinetic, 'Mutational, and Structural Analysis of Malonate Semialdehyde Decarboxylase from\r Coryneform\r Bacterium Strain FG41: Mechanistic Implications for the Decarboxylase and Hydratase Activities', *Biochemistry*. **2013**, *52*, 4830-4841.

[33] H. Li, S. Chen, X. H. Peng, J. G. Sun,C. Y. Shu, L. Jiang, C. R. Wang, 'Nanosci. Biocompatibility Assessment of Polyethylene Glycol-Poly L-Lysine-Poly Lactic-Co-Glycolic Acid Nanoparticles In Vitro and In Vivo', *Nanotechnol*. **2016**, *16*, 2504-2508.

[34] M. H. Chen, P. Li, D. Y. Hu, Z. Song, T. T. Li, L. H. Jin, W. Xue, B. A. Song, 'Antibacterial activities against rice bacterial leaf blight and tomato bacterial wilt of 2-mercapto-5-substituted-1,3,4-oxadiazole/thiadiazole derivatives', *Bioorg. Med. Chem. Lett*. **2016**, *26*, 168-173.

[35] Z. W. Chen, P. Li, D. Y. Hu, L. G. Dong, J. K. Pan, L. Z. Luo, W. Y. Zhang, W. Xue, L. H. Jin, B. A. Song, 'Synthesis, antiviral activity, and 3D-QSAR study of novel chalcone derivatives containing malonate and pyridine moieties', *Arab. J. Chem*. **2015**, *5*, 3-15.

[36] Isabelle, T. Christophe, N. Stéphane, N. Lamiaa, A. M. A. Ludivine, L. Rabab, F. Céline, A. Magali, G. B. Marwan, K. Fabrice, O. 'Synthesis and Anticancer Activity of Gold Porphyrin Linked to Malonate Diamine Platinum Complexes', *Inorg. Chem*. **2019**, *58*, 12395-12406.

[37] S. T. Zhang, K. Cheng, X. H. Wang, H. Yin, 'Selection, synthesis, and anti-inflammatory evaluation of the arylidene malonate derivatives as TLR4 signaling inhibitors', *Bioorg. Med. Chem*. **2012**, *20*, 6073–6079.

[38] J. Zhang, F. Yang, Z. T. Qiao, M. Y. Zhu, H. C. Zhou, 'Chalcone benzoxaborole hybrids as novel anticancer agents', *Bioorg. Med. Chem. Lett*. **2016**, *26*, 5797–5801.

[39] D. D. Cao, G. S. Fang, J. X. Zhang, H. Y. Wang, C. W. Zheng, G. Zhao, 'Enantioselective Michael Addition of Malonates to Chalcone Derivatives Catalyzed by Dipeptide-derived Multifunctional Phosphonium Salts', *J. Org. Chem*. **2016**, *81*, 9973–9982.

[40] X. Wang, P. Li, Z. N. Li, J. Yin, M. He, W. Xue, Z. W. Chen, B. A. Song, 'Synthesis and bioactivity evaluation of novel arylimines containing a 3-aminoethyl-2-(p-trifluoromethoxy) anilino-4(3H) -quinazolinone moiety', *J. Agric. Food Chem*. **2013**, *61*, 9575–9582.

[41] P. Li, D. Y. Hu, D. D. Xie, J. X. Chen, L. H. Jin, B. A. Song, 'Design, synthesis, and evaluation of new sulfone derivatives containing a 1,3,4-oxadiazole moiety as active antibacterial agents', *J. Agric. Food Chem*. **2018**, *66*, 3093–3100.

[42] X. H. Ruan, C. Zhang, S. C. Jiang, T. Guo, R. J. Xia, Y. Chen, X. Tang, W. Xue, 'Design, synthesis, and biological activity of novel myricetin derivatives containing amide, thioether, and 1,3,4-thiadiazole moieties', *Molecules*. **2018**, *23*, 3132–3142.

[43] Y. Y. Wang, F. Z. Xu,Y. Y. Zhu, B. A. Song, D. X. Luo, G. Yu, S. H. Chen, W. Xue, J. Wu, 'Pyrazolo[3,4-d]pyrimidine derivatives containing a Schiffff base moiety as potential antiviral agents', *Bioorg. Med. Chem. Lett*. **2018**, *28*, 2979–2984.

[44] Z. X. Wu, J. Zhang,J. X. Chen, J. K. Pan,L. Zhao,D. Y. Liu,A. W. Zhang, J. Chen, D. Y. Hu, B. A. Song, 'Design, synthesis, antiviral bioactivity and three-dimensional quantitave structure-activity relationship study of novel ferulic acid ester derivatives containing quinazoline moiety', *Pest. Manag. Sci*. **2017**, *73*, 2079–2089.

[45] L. J. Chen, T. Guo, R. J. Xia, X. Tang, Y. Chen, C. Zhang,W. Xue, 'Novel Phosphorylated Penta-1,4-dien-3-one Derivatives:Design, Synthesis, and Biological Activity', *Molecules*. **2019**, *24*, 925-937.

[46] J. Chen, J. Shi, L. Yu, D. Liu, X. H. Gan, B. A. Song, D. Y. Hu, 'Design, synthesis, antiviral bioactivity and defense mechanisms of novel dithioacetal derivatives bearing a strobilurin moiety', *J. Agric. Food Chem*. **2018**, *66*, 5335–5345.

[47] X. Y. Li, J. Liu, X. Yang, Y. Ding, J. Wu,D. Y. Hu, B. A. Song, 'Studies of binding interactions between dufulin and southern rice black-streaked dwarf virus P9-1', *Bioorg. Med. Chem*. **2015**, *23*, 3629–3637.

10.1002/cbdv.202000025

Chem. Biodiversity